

## FATIGUE LIFE OF CONSTRUCTIONAL MATERIALS UNDER BENDING WITH TORSION FOR CRACK PROPAGATION

G. Gasiak, G. Robak

*Opole University of Technology, ul. St. Mikołajczyka 5, 45-271 Opole, Poland*

**Abstract** The paper presents description of the equivalent range of the stress intensity factor in the case of bending with torsion of specimens where initiation and propagation of fatigue cracks are observed. Calculations with the Matlab-Simulink program were performed in order to estimate fatigue life. The calculations were realized for variable amplitudes of the resultant moment 13 and 16 N·m. The Forman's relation was also used for the calculations. It has been shown that the Forman's relation is suitable for description of fatigue life in the tested range of fatigue crack propagation.

### 1. Introduction

Stress intensity coefficients are often applied for description of the stress state in elements of structures where fatigue cracks occur and develop [1-2]. They are used in many relationships describing crack propagation rate or fatigue life in the range of fatigue crack propagation [3]. The known relationships for fatigue life estimation usually use stress intensity coefficients under simple loading states [4]. Under complex loading states, for example bending with torsion, it is necessary to determine the equivalent value of the stress intensity factor, including all the components of stress occurring in the loaded element [5]. Thus, the existing relationships describing fatigue life should be verified.

The authors of this paper try to describe the equivalent range of the stress intensity factor in the case when a specimen is simultaneously loaded by the torsional and bending moments. Next, fatigue life is going to be estimated in the range of fatigue crack propagation. The Forman's relation is used for estimation.

### 2. The tests

The tests were performed at the fatigue test stand MZGS-100. At this stand, it is possible to realize courses, variable in cycles, under bending, torsion and combined bending with torsion. The test results have been presented in [6]. The tests were done for two amplitudes of the resultant moment,  $M_{aw0} = 13$  and  $16$  N·m. A scheme of the specimen loading has been shown in Fig. 1 [6]. For calculations, it was assumed that the amplitude of the resultant moment  $M_{aw0}$  changed together with the propagating crack. That change was caused by a change of the specimen rigidity while fatigue crack propagation [7].

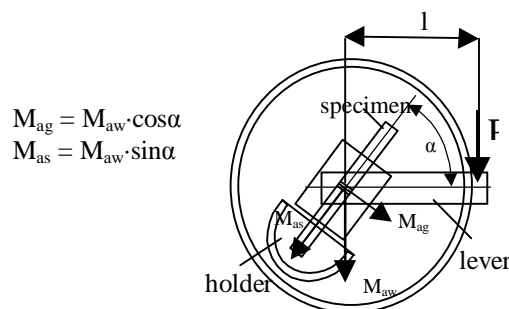


Fig. 1 A scheme of specimen loading

### 3. Description of the stress state

Fig. 2 shows stress distribution on the plane of fatigue crack propagation in the specimen, caused by bending and torsional loading.

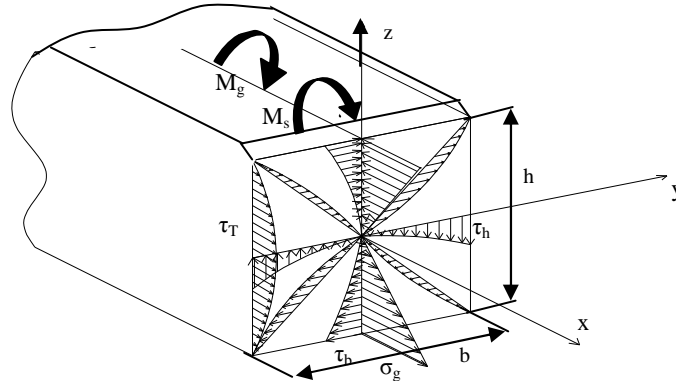


Fig. 2 Stress distribution in the specimen section, i.e. on the plane of fatigue crack propagation;  $\tau_s = \tau_b > \tau_h$  – shear stresses caused by the torsional moment,  $\tau_T$  – shear stress caused by shearing force,  $\sigma_g$  – normal stress caused by the bending moment

Normal stresses,  $\sigma_g$  and shear stresses,  $\tau_s$  and  $\tau_T$ , used for determination of the stress intensity factor are expressed as

$$\sigma_g = \frac{6M_{aw} \cos \alpha}{b(h-a)^2}, \quad (1)$$

$$\tau_s = \tau_b = \frac{M_{aw} \sin \alpha}{k_2 b(h-a)^2}, \quad (2)$$

$$\tau_T = \frac{P}{A}, \quad (3)$$

where  $M_{aw0} = P \cdot l$ ,  $P$  – loading force for  $M_{aw0} = 13 \text{ N} \cdot \text{m}$  equal to 65 N and  $M_{aw0} = 13 \text{ N} \cdot \text{m}$  equal to 80 N,  $l$  – lever length,  $a$  – actual length of crack,  $b$  – specimen width,  $h$  – specimen height,  $k_2$  – coefficient depending on the ratio  $b / (h-a)$  [7],  $A$  – section area of the specimen in the place of notch.

In description of fatigue crack propagation a range of the stress intensity factor was applied. It was defined from [8]:

$$\Delta K_{eq} = \sqrt{\Delta K_I^2 + \Delta K_{II}^2 + \frac{1}{(1-\nu)} \Delta K_{III}^2}, \quad (4)$$

where:  $\Delta K_I$ ,  $\Delta K_{II}$ ,  $\Delta K_{III}$  – ranges of stress intensity coefficients for loading modes I, II and III.

From analysis of the stress state in the specimen it appears that the stress  $\tau_T$  causing longitudinal shearing is very low in comparison with stresses  $\sigma_g$  and  $\tau_s$  ( $\tau_T \approx 1\%$  of  $\sigma_g$ ) and it does not strongly influence the process of fatigue crack development, so  $\Delta K_{II} = 0$  is assumed for further considerations.

The equivalent range of stress intensity factor takes the form:

$$\Delta K_{eq} = \sqrt{\Delta K_I^2 + \frac{1}{(1-\nu)} \Delta K_{III}^2}, \quad (5)$$

where:

$$\Delta K_I = M_{K_I} \Delta \sigma_g \sqrt{\pi a}; [1],$$

$$\Delta K_{III} = M_{K_{III}} \Delta \tau_s \sqrt{\pi a}; [1],$$

$$M_{KI} - \text{correction coefficient} \quad M_{KI} = \frac{5}{\sqrt{20 - 13\frac{a}{h} - 7\left(\frac{a}{h}\right)^2}} \quad [11],$$

$$M_{KIII} - \text{correction coefficient} \quad M_{KIII} = \sqrt{2\frac{h}{a} \operatorname{tg}\left(\frac{\pi a}{2h}\right)} \quad [10].$$

#### 4. Estimation of fatigue life

The Forman's relation [9] was used for fatigue life estimation. The equivalent range of stress intensity factor in the form [5]:

$$\frac{da}{dN} = \frac{C(\Delta K_{eq})^m}{(1-R)K_C - \Delta K_{eq}} \quad (6)$$

was introduced to the Forman's relation.

After integration of Eq. (6), we obtain the following relation for fatigue life estimation:

$$N = \int_{a_0}^{a_i} \frac{(1-R)K_C - \Delta K_{eq}}{C_1(\Delta K_{eq})^{m_1}} da, \quad (7)$$

where:  $R = -1$ ,  $K_C = K_{IC} = 259 \text{MPa} \cdot \text{m}^{0.5}$

Parameters  $C_1$  and  $m_1$  from Eq. (7) were calculated on the basis of test results, assuming the criterion of the maximum accuracy of theoretical curve fitting to the experimental points with the method of least squares of the distance from the theoretical curve. The same scale of axes of the normalized coordinate system was assumed in relation of the test data range. A distance between the experimental points and the theoretical curve was defined as minimum of the length of interval  $d_i$  [8] joining the experimental point  $M_i$  and the theoretical curve  $\Gamma$  (Fig.3).

$$d_i = \sqrt{\left(\frac{a_{\text{exp}_i} - a_{\text{obl}_i}}{a_{\text{exp}_i}^{\text{max}}}\right)^2 + \left(\frac{N_{\text{exp}_i} - N_{\text{obl}_i}}{N_{\text{exp}_i}^{\text{max}}}\right)^2} \quad (8)$$

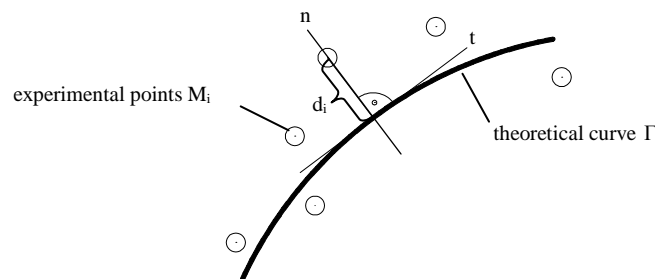


Fig. 3 Distance  $r_i$  between experimental points  $M_i$  and the curve  $\Gamma$

Eqs. (6) and (7) were solved with simulation methods and the Matlab-Simulink program. Values of the parameters  $C_1$  and  $m_1$ , and life  $N_{\text{obl}}$  are presented in Table 1.

Table 1. Values of the parameters  $C_1$ ,  $m_1$  and life  $N_{cal}$ 

Material	$M_{aw0}$ [N·m]	Ratio $M_{ag}/M_{as}$	$C_1$	$m_1$	$N_{cal}$ [cycles $\cdot 10^5$ ]
18G2A	13	$M_{as} = 0$	$0,186 \cdot 10^{-3}$	1,20	2,41
		7,59	$0,164 \cdot 10^{-3}$	1,21	2,93
		3,73	$0,117 \cdot 10^{-3}$	1,24	3,50
		2,41	$0,165 \cdot 10^{-3}$	1,04	4,47
		1,73	$0,154 \cdot 10^{-3}$	0,95	6,11
		1,30	$0,235 \cdot 10^{-4}$	1,56	6,86
		1,00	$0,456 \cdot 10^{-4}$	1,31	8,05
	16	$M_{as} = 0$	$0,205 \cdot 10^{-3}$	1,18	1,51
		7,59	$0,140 \cdot 10^{-3}$	1,36	1,58
		3,73	$0,160 \cdot 10^{-3}$	1,26	1,79
		2,41	$0,331 \cdot 10^{-3}$	1,00	1,97
		1,73	$0,381 \cdot 10^{-4}$	1,66	2,58
		1,30	$0,210 \cdot 10^{-3}$	1,00	3,16
		1,00	$0,226 \cdot 10^{-3}$	0,90	4,01

### 5. Analysis of the calculation results

Figs. 4 and 5 show the graphs of the experimental and calculation lives,  $N_{exp}$  and  $N_{cal}$ , versus the crack length  $a$ . The solid line means lives  $N_{cal}$  calculated from Eq. (7), and the points express experimental lives  $N_{exp}$  for three specimens. It can be seen that as the fatigue crack length  $a$  increases, difference between experimental and calculation results becomes greater. The maximum difference between  $N_{exp}$  and  $N_{cal}$  for loading by amplitude of the resultant moment  $M_{aw0} = 13$  N·m does not exceed 11% (Fig. 4d). Under loading by the resultant moment  $M_{aw0} = 16$  N·m, this difference does not exceed 15% (Fig. 5a).

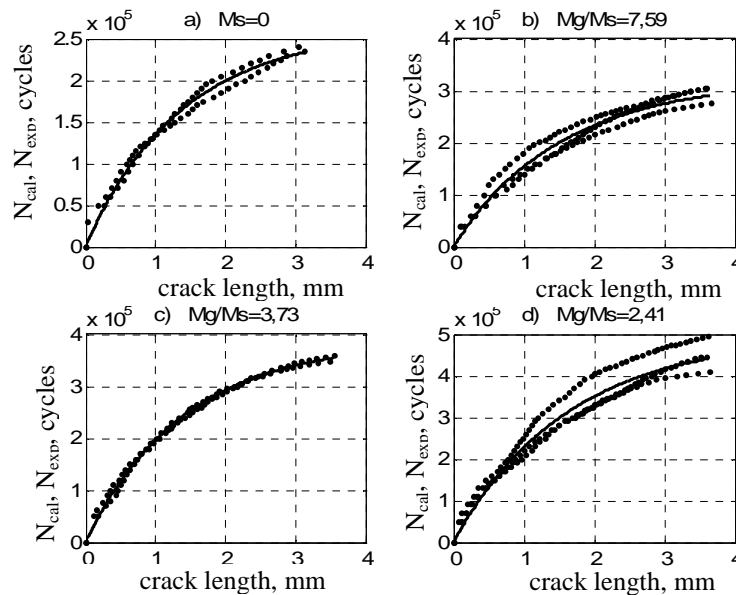


Fig. 4 Graphs of the experimental and calculation lives,  $N_{exp}$  and  $N_{obl}$ , versus the crack length,  $a$ , for 18G2A steel and amplitude of the resultant moment  $M_{aw0} = 13$  N·m for ratios  $M_{ag}/M_{as}$ : a)  $M_{as} = 0$ , b) 7.59, c) 3.73, d) 2.41

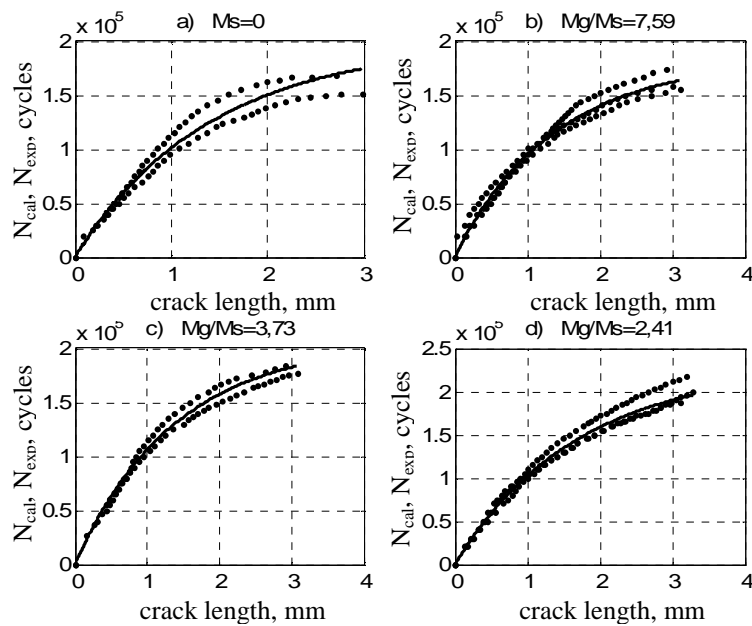


Fig. 5 Graphs of the experimental and calculation lives,  $N_{exp}$  and  $N_{obl}$ , versus the crack length,  $a$ , for 18G2A steel and amplitude of the resultant moment  $M_{aw0} = 16 \text{ N}\cdot\text{m}$  for ratios  $M_{ag}/M_{as}$ : a)  $M_{as} = 0$ , b) 7.59, c) 3.73, d) 2.41

Figs. 6 and 7 present comparison of the calculated and experimental lives,  $N_{obl}$  and  $N_{exp}$ . The maximum values of the experimental life are determined for critical lengths of fatigue cracks  $a_{kr}$ . Above the critical lengths, it is not possible to use stress description in order to determine the fatigue life because of high plasticization of the material. The given values are included into the interval  $a_{kr} = 3.45 \div 3.66 \text{ mm}$  for loading amplitude  $M_{aw0} = 13 \text{ N}\cdot\text{m}$ , and  $a_{kr} = 2.92 \div 3.23 \text{ mm}$  for loading amplitude  $M_{aw0} = 16 \text{ N}\cdot\text{m}$  and the depend on the ratio  $M_{ag}/M_{as}$ .

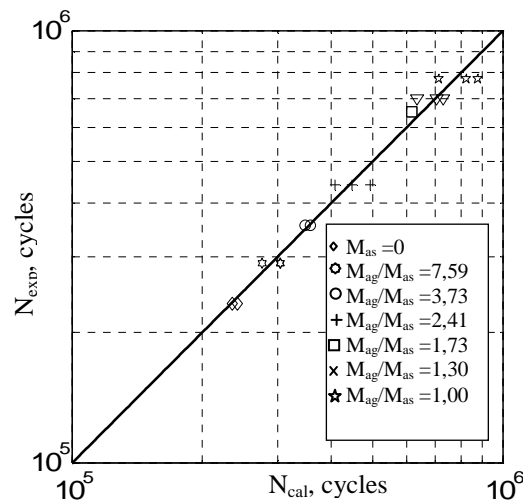


Fig. 6 Comparative graph for experimental and calculated lives,  $N_{exp}$  and  $N_{cal}$ , for amplitude of the resultant moment  $M_{aw0} = 13 \text{ N}\cdot\text{m}$

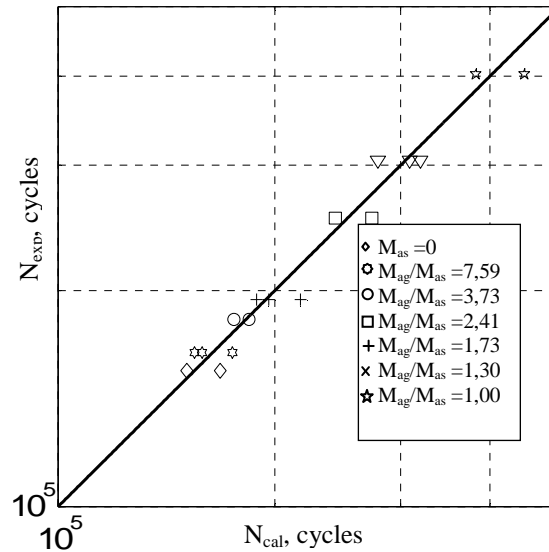


Fig. 7 Comparative graph for experimental and calculated lives,  $N_{exp}$  and  $N_{cal}$ , for amplitude of the resultant moment  $M_{aw0} = 16 \text{ N}\cdot\text{m}$

It can be seen that under both loading amplitudes the results are included into a narrow scatter band. Thus, the applied Forman's relation and the equivalent range of stress intensity factor (5) allow to obtain good conformity of the results. In this order, the coefficients  $C_1$  and  $m_1$  should be determined from the experimental data. The least conformity is observed for ratios  $M_{ag} / M_{as} = 1.30$  and  $1.00$  for both considered moment amplitudes.

## 6. Conclusions

From the performed calculations and their analysis the following conclusions can be drawn:

1. The relation describing fatigue life based on the Forman's relation and including the equivalent range of stress intensity factor  $\Delta K_{eq}$  provides suitable estimation of fatigue life of specimens made of 18G2A steel.
2. In order to estimate fatigue life with Eq. (7) it is necessary to determine coefficients  $C_1$  and  $m_1$ , depending on material properties and the ratios of amplitudes of bending and torsional moments.

## References

1. Kocańda S.: Fatigue cracks in metals (Polish). WNT, Warszawa 1985
2. Neimitz A.: Fracture mechanics (Polish). PWN, Warszawa, 1998
3. Gasiak G.: Life of constructional materials under cyclic loading with participation of the load mean values (Polish). Oficyna Wyd. PO, Opole 2002
4. Achtelik H., Gasiak G., Grzelak J.: Experimental verification of life models for flat specimens with central notches, subjected to variable tension (Polish). XXI Sympozjum Mechaniki Eksperymentalnej Ciała stałego, Oficyna Wyd. PW, 13-16 października, Jachranka, 2004 s. 117-122
5. Socie D. F., Hua C. T., Worthem D. W.: Mixed mode small crack growth. Fatigue and Fracture of Engineering Materials and Structures Vol. 10, 1987, pp. 1-16
6. Gasiak G., Robak G.: Determination of fatigue life of 10HNAP and 18G2A steels in the range of initiation and propagation of fatigue cracks under bending with torsion (Polish). X Konferencja Mechaniki Pękania, Wisła, 11-14 września 2005, Zeszyty Naukowe PO, Mechanika Nr 304, z 82, Opole 2005.

7. Gasiak G., Grzelak J., Robak G. Simulation of life within fatigue crack development under bending with torsion (Polish). X Konferencja Mechaniki Pękania, Wisła, 11-14 września 2005, Zeszyty Naukowe PO, Mechanika Nr 304, z 82, Opole 2005.
8. In – Tae Kim: Weld root crack propagation under mixed mode I and III cyclic loading. Engineering Fracture Mechanics Vol. 72, 2005, pp. 523-534.
9. Forman R. G., Kearney V. E., Engle R. M.: Numerical analysis of crack propagations in cycling – loaded structures. J. Basic Engng. Sept. 1967, pp 4569-463
10. Hellier A. K., Corderoy D. J. H., McGirr M. B.: A practical mixed mode II/III fatigue test rig. International Journal Fatigue Vol. 9, 1987, pp. 95-101
11. Pickard A. C.: The application of 3 – dimensional finite element methods of fracture mechanics and fatigue life predictions. London, 1986

*Praca naukowa finansowana ze środków na naukę w latach 2005/2006 jako projekt badawczy. Praca współfinansowana z Europejskiego Funduszu Społecznego Unii Europejskiej i budżetu państwa*

